Liquefaction optimization of grape pulp using response surface methodology for biopolyol production and bio-based polyurethane foam synthesis

Furkan ÇOLAKOĞLU[1], Emre AKDOĞAN[1], Murat ERDEM[1,*]

[1]Department of Chemistry, Faculty of Science, Eskisehir Technical University, Eskisehir, Turkey

*Correspondence: merdem@eskisehir.edu.tr

ORCIDs:

https://orcid.org/0009-0000-5524-7332 (Furkan Çolakoğlu)

https://orcid.org/0000-0003-1505-9323 (Emre Akdoğan)

https://orcid.org/0000-0003-3601-3316 (Murat Erdem)

Abstract: Both environmental and economic disadvantages of using petroleum-based products have been forcing researchers to work on environmentally friendly, sustainable, and economical alternatives. The purpose of this study is to optimize the solvothermal liquefaction process of grape pomace (GP) using response surface methodology (RSM) coupled with a central composite design (CCD). After investigating the physicochemical properties of the liquified products (biopolyol) in detail, a bio-based rigid polyurethane foam (RPUF) was synthesized and characterized. The hydroxyl and acid numbers and viscosity values of all the biopolyols were analyzed. According to variance analysis results (%95 confidence range), both the reaction temperature and catalyst loading were determined as significant parameters on the liquefaction yield (LY). The model was validated experimentally in the reaction conditions which are 4.25% catalyst loading, 50 min reaction time, and 165 °C reaction temperature, which yields an LY of 81.3%. The biopolyols produced by the validation experiment display similar characteristics

(hydroxyl number 470.5 mg KOH/g, acid number 2.31 mg KOH/g, viscosity 1785 cP at 25 °C) to those of commercial polyols widely preferred in the production polyurethane foam. The physicochemical properties of bio-based foam obtained from the biopolyol were determined and the thermal conductivity, closed-cell content, apparent density, and compressive strength values of bio-based RPUF were 31.3 mW/m·K, 71.1%, 33.4 kg/m^3, and 105.3 kPa, respectively.

Key words: Hardaliye, grape pulp, biopolyol, bio-based rigid polyurethane foam, design of experiment

1. Introduction

The use of petroleum as an energy source results in harm to the natural environment. Their damages are also increasing over time because of the global energy consumption needed with the increasing world population. Therefore, researchers have been led to look for an alternative, environmentally friendly, and sustainable products. The use of industrial and agricultural biomass residues as bio-based raw materials has great potential in terms of renewable energy sources. Biomasses are highly abundant, accessible, and renewable resources that can easily be converted into different types of high-value materials. Agricultural biomass, produced by photosynthesis by using carbon dioxide (CO_2) in the atmosphere, has a shorter generation time, unlike fossil fuels. Besides, biomasses are considered as "carbon neutral" fuel because when biomass burns, it releases CO_2 that it absorbed from the atmosphere [1].

To evaluate the biomasses, the conversion into precious products by various liquefaction methods can be considered using the appropriate reaction routes. Acid-catalyzed solvothermal liquefaction (ACSL) is the mostly used method to liquefy biomasses for one of the components in the formation of polyurethane foam. Biomasses are usually produced in a mixture of polyhydric alcohols as a liquefaction solvent for processes where the amount of catalyst, reaction temperature, and time are variable in ACSL [2, 3]. Several researchers have lately produced biopolyols derived from the liquefaction of various lignocellulosic biomass to create bio-based RPUFs, such as spent coffee grounds [4], cork powder [5], cotton stalk [2], banana bamboos [6], cotton burrs [7], wheat straw [8], peanut shells [9].

~~The production of grapes and its goods has a very important place for the inhabitants of the region in the Thrace Region, which has made a name for itself with its viticulture~~

practices. Hardaliye is a nonalcoholic beverage produced from grapes, mustard seeds, and sour cheery leaves [10, 11]. After producing Hardaliye, the grape pulp (GP) is the residuum left. The cost of GP is rather low and the pulp is generally thrown away or neglected; however, due to the lignocellulosic content, the GP is a good candidate which can be converted into renewable biopolyol.

The grape is one of the largest fruit crops in Turkey. According to the Ministry of Agriculture and Forestry of the Republic of Turkey, 4.1 million tons of grapes were produced in Turkey over an area of 420,000 hectares during the 2020 production period [10]. About 60% of the world's grape production is used to make wine and similar beverages, and this processing can produce a large amount of grape pomace, which consists of grape skins, stems, and seeds. Grape pomace contains cellulose, hemicellulose, lignin, protein and phenolic compounds. The higher lignocellulose content can have a positive effect on the utilization of grape pomace [11]. Shao et al. optimized four liquefaction factors and successfully liquefied grape seeds in the mixed solvent of polyethylene glycol 400 and glycerol for biopolyol production [12]. Nevertheless, the study on liquefaction of GS to produce biopolyol and polyurethane foam is rarely reported.

Polyurethanes are high-performance polymers formed by polycondensation reactions of polyols and diisocyanates. Polyurethanes are frequently used in making thermoplastics, elastomers, foams, paints, adhesives, and rubber. Rigid polyurethane foam (RPUF) is one of the most used types of polyurethane. Heat and sound insulation are important application areas of RPUFs [13]. The types of isocyanates and polyols used in the RPUF formulation greatly affect the properties of foams. In addition, the massive use of commercial polyols for RPUF synthesis poses various economic and environmental

problems. In this context, due to increasing concerns associated with petroleum use, the biopolyols produced from GP via liquefaction technique seem a striking alternative to commercial petroleum-based polyols [3].

There are numerous studies on the conversion of different agricultural crop residues into valuable biopolyols; however, to the best of our knowledge, this is the first study to evaluate GP via the ACSL using experimental design for biopolyol and polyurethane production. In the present study, solvothermal liquefaction of GP was performed by using 20 wt% glycerol and 80 wt% PEG400 solvent mixture in the presence of sulfuric acid as a catalyst. The effects of the reaction time, reaction temperature, and catalyst loading on the LY were investigated to optimize LY using an RSM coupled with CCD. Finally, RPUF was produced using a one-shot method with half substation of GP-based biopolyol with the commercial polyol. The produced bio-based RPUF was characterized via SEM, FT-IR spectroscopy, gas displacement pycnometer, universal test machine, and heat flow meter.

2. Materials and Methods

2.1. Materials

GP was provided from Kırklareli Rumeli Hardaliyesi Factory. ~~For the synthesis and characterization of biopolyol and RPUF,~~

Polyethylene glycol 400 (PEG 400) and glycerol (G) were purchased from Tekkim Kimya. Sulfuric acid (SA), 1,4-dioxane, sodium hydroxide (NaOH), phthalic anhydride pyridine, imidazole, ethyl alcohol, toluene, acetone, potassium hydrogen phthalate, silicon oil (Rhodorsil Oils 47), tetramethyl ethylenediamine, dibutyltin dilaurate, and barium chloride were reagent grade and purchased from Sigma-Aldrich. pMDI (polymethylene diphenyl isocyanate), surfactant (Tegostab B 8476), and petroleum-based

polyol were provided by Ravago Petrokimya Üretim A.Ş. The distilled water which is a chemical blowing agent was produced in our laboratory.

2.2. Methods

2.2.1. Pretreatment of GP

After drying GP residues at a temperature of 70 °C until reaching the constant weight in an oven, the residues were ground and sieved below 250 μm.

2.2.2. Solvothermal liquefaction of GP

The ACSL method was carried out in accordance with the literature [14]. The liquefaction reaction was stirred in a 250 ml of reaction flask with an overhead stirrer. The mixture of liquefying solvent was formed with 20 wt% glycerol and 80 wt% PEG400 and the liquefying solvent/GP ratio was fixed at 4/1 (wt/wt). The amount of sulfuric acid (SA) was adjusted according to the amount of liquefaction solvent mixture. Before starting the reaction, GP powder (5.0g) and liquefying solvent (20g) were mixed for 3 min, then placed in a preheated silicon oil bath. After reaching the reaction mixture to the desired temperature (150-180 °C), SA was immediately poured into the flask. The reaction was continued for the specified times at 200 rpm. After the reaction time (20-100 min) was over, the mixture was placed in a cold-water bath to quench the reaction. The mixture was then diluted with 100 ml of solution, containing 80 mL of 1,4-dioxane and 20 mL of water, and kept stirring for 1 h. The diluted mixture was filtered via suction filtration to isolate the residue. The insoluble residue dried until reaching the constant weight in a laboratory oven at 105 °C. The solvent was evaporated using a rotary evaporator to obtain biopolyol. The LY was calculated as Equation 1.

$$LY(\%) = \frac{Y_2 \times 100}{Y_1} \quad (1)$$

2.2.3. Experimental design and process optimization

It is very important to detect the variability of the parameters affecting the LY in order to increase efficiency with fewer experimental studies. At this point, CCD of RSM is one of the preferred applications to study the effects of different variables on the targeted response.

Table 1

Minitab ® 19 statistical software was used to determine the effects of reaction parameters such as catalyst loading (X_1), reaction time (X_2), and reaction temperature (X_3) on the LY (Table 1). The effects of the three independent variables on LY and the experimental design matrices with coded and real values corresponding to the results of LY are shown in Table 2. A total of 17 experiments were performed to obtain both biopolyols and the LY values. The relationships between the obtained experimental and predicted data were analyzed with a 95% confidence level analysis of variance. The accuracy and reliability of the created model were examined with the correlation coefficient (R^2). Minitab software was used to visualize response surface and contour plots.

Table 2

2.2.4. Characterization of the biopolyols

The hydroxyl and acid numbers of biopolyols were determined by ASTM D 4274 (Method D) and ASTM D 4662 test standards, respectively. Viscosities of biopolyols at 25 °C were determined with the Brookfield DV3T Viscometer, following the ASTM D 4878-08 standard. The chemical structures of the biopolyols were analyzed using the

ATR mode of the FT-IR spectrometer over a scan range of 4000-700 cm^{-1}. Molecular weight analysis of biopolyol was performed using a gel permeation chromatography (Agilent Technology) equipped with a refractive index detector (G1362A) and a GPC column (TSK G3000 PWXL). Tetrahydrofuran was used as the mobile phase at a flow rate of 1.0 mL/min, column temperature of 35°C under 10.0 MPa pressure. The average molecular weight of the samples was calculated using a calibration curve of monodisperse polystyrene standards.

2.2.5. Preparation of RPUF

RPUFs were fabricated with a one-shot and free-foaming method. The bio-based RPUF was synthesized using the biopolyol which is produced from the optimum ACSL reaction condition, and petroleum-based polyol was partially substituted with biopolyol in the ratio of 1:1. (Table 3). The polyol mixture containing polyols, water, catalysts, and surfactant was placed in a 500 mL syringe in an appropriate amount and mixed with a mechanical stirrer at 2000 rpm for 2 min. At the end of mixing, pMDI was swiftly added to the mixture with another syringe while the stirring was continued. After the foam mixture reached the creamy phase (5-8 s), the mixture was rapidly poured into a metal mold with dimensions of 21cm×21cm×7cm (length, width, thickness). After the formation of foam was completed, it was removed from the mold and left to cure for 3 days.

Table 3

2.2.6. Characterization of RPUF

The measurement of the thermal conductivity of the foams, cut into dimensions of 20cm×20cm×3cm, was carried out using the Linseis HFM 300 Heat Flow Meter

regarding ASTM C518 standard. While the temperature of the upper plate was adjusted to 38°C, the lower one was adjusted to 10°C, keeping the average foam temperature at 24°C.

To determine their closed cell contents and apparent densities, three pieces of the foams were used in dimensions of 3cm×3cm×3cm. The final dimensions of each of the pieces were measured with a caliper to calculate the apparent density. The closed cell contents were then determined using a gas displacement pycnometer (Micromeritics AccuPyc II 1340) according to ASTM D-6226. The average value of the results was reported.

The measurement of compressive strength values was determined with three pieces, cut into dimensions of 5cm×5cm×3cm, using the universal testing machine (Zwick/Roell brand Proline) according to ASTM D-1621 test standard at room temperature. Compressive stress at 10% strain was applied to the foams and the strength values were detected at this deformation. The average values of the results were given.

Morphological characterization of RPUFs was performed using Scanning Electron Microscopy (SEM, Carl Zeiss Ultra Plus, Oberkochen, Germany) using an appropriate voltage at 100x magnification. The sliced foam pieces were coated with gold to have a conductive layer.

3. Results and Discussion

3.1. Statistical analysis

3.1.1. Experimental design

In the presented study, the process of obtaining biopolyol from GP by ACSL was optimized to increase the percentage of LY based on 3 different experimental parameters to prevent both economic and time loss. Table 2 displays the experimental CCD matrix for the production of biopolyols along with the corresponding responses. It was detected

that LY values diversified between 59.35% and 88.99% according to the liquefaction reaction conditions. When the reaction conditions are 180 °C, 60 min, and 4 wt% catalyst loading, the highest LY value (86.17%) was achieved. This result revealed that ACSL is an efficient and feasible way to convert GP to biopolyol. A quadratic polynomial equation was developed so that the correlation between LY and reaction parameters in terms of coded values from the model explains. The relevant equation is presented in Equation 2.

$$Y_{LY} = 77.15 + 5.27X_1 + 2.50X_2 + 4.81X_3 - 1.51X_1^2 + 0.14X_1X_3 - 1.48X_2X_3 \quad (2)$$

where Y_{LY} is the liquefaction yield (%), X_1 is the catalyst loading, X_2 is the reaction time (min), and X_3 is the reaction temperature (°C). The positive coefficients cause the LY values to increase, whereas the negative coefficients cause the LY values to decrease in the studied range. While the model was created, incorrect responses can be obtained due to operational errors. These values can be considered as outliers and they can be extracted from the model in order to better analyze the experimental results; therefore, to obtain a more robust model, experiment number 2 was detected as an outlier and removed from the model.

The variance analysis (ANOVA) results of the obtained quadratic model were tabulated in Table 4. According to the F-test, the F value of the quadratic model was detected at 104.55 with a low probability value (p-value <0.001). This result indicates that the obtained model is quite significant. A p-value is used as a measure of the statistical significance of research results and when the p-value is lower than 0.05, the research results are generally considered to be statistically significant. In this case, the model terms of X_1, X_2, X_3, X_1^2, X_1X_3, and X_2X_3 were significant. The remaining terms were not considered insignificant because p-values were greater than 0.005. The p-value of the lack of fit was found to be 0.450, which is not statistically significant. This implies that the

experimental error at the center point (experiment numbers 9,10, and 17) of the model is in the acceptable range, and the predicted results are convincing [15]. The regression coefficient was 0.9859, which was close to 1. It is also implied that the experimental data for the liquefaction reactions fitted well with the predicted value of the model [16].

Table 4

3.1.2. Optimization of ACSL parameters

Contour and three-dimensional (3D) surface plots were drawn using Minitab software according to the quadratic regression equation and shown in Figure 1-3. While the combined effects of two particular factors were examined, the remaining factor was kept constant at the center point (0 level in Table 1) in these figures.

Figures 1a and b show 3D response surface and contour plots depicting the effects of catalyst loading and reaction time on the liquefaction yield. LY reached its maximum value in the range of 5-6% catalyst loading and 60-100 min of reaction time. Beyond those critical points, the LY showed a tendency to decrease. The recondensation reaction in the depolymerized lignocellulosic content of GP might be the reason behind this decrease in the LY value, as reported by other researchers [17-19]. In accordance with Figure 1b, it can be said that to obtain an LY value of 85% and above, one can set up reaction conditions in which the reaction time and the catalyst loading were greater than 86.1 min and 4.7%, respectively.

Figure 1

Figure 2a and b show the combined effects of reaction time and temperature on the LY values. The effect of reaction temperature was greater than the reaction time on the increase in the LY value. The conversion of GP increased to 86.43% when the reaction temperature was boosted from 140 °C to 180 °C. To reach the LY value of more than 85% at the minimum reaction time (for example 20 min), the reaction temperature should be at least 176.4 °C. Furthermore, when Figure 3a and b are examined, the increase in the catalyst loading improved the LY value. It can also be shown for reaching the LY value of 90% that the reaction temperature and catalyst loading were required to be greater than 171 °C and 4.4%, respectively.

Figure 2

Figure 3

As a result, the optimal reaction conditions were estimated for the conversion of GP into biopolyol using Minitab software. The optimal reaction parameters of ACSL for the conversion of GP were detected as 4.25% catalyst loading, 50 min reaction time, and 165 °C reaction temperature, resulting that an LY value of 80.1%. In the presented study, these optimal values were chosen so that the energy and time consumption is low, and the obtained biopolyols display fine properties for the production of polyurethanes.

3.1.3. Validation of the model

In order to validate the model, the validation experiments on the optimal reaction conditions were performed three times with the same procedure and Table 5 illustrates the results of the experiments. While the experimental LY value was 81.3%±1.5, the LY

value for the selected target estimate was 80.1%. The error was found to be less than 1.5% which indicates that the proposed model was in excellent agreement with those predicted reaction conditions. As a result, the obtained model was highly accurate and reproducible.

Table 5

3.2. Physicochemical properties of obtained biopolyols

The goal of this study was to convert GP formed after the production of Hardaliye into biopolyols according to the concept of biorefinery. It was demonstrated that GP, which is released every year as a waste of the beverage industry, has a huge potential for conversion into biopolyols, one of the most important components of polyurethane. Besides, the properties of biopolyols are of significance to investigate their potential use in polyurethane production. To that end, their hydroxyl and acid numbers, and viscosity values were evaluated. While Shao et al. used grape seeds as biomass, we liquified grape pulp. In addition to seeds, pulp also contains the other components of grape herb/fruit. So, both chemical composition and behavior in the conversion process of two kinds of biomass are different. In this case, it is expected that the properties of these biopolyols obtained from different studies will differ from each other. In 2016, Shao et al. evaluated the feasibility of liquefying grape seeds for the production of biopolyol. On the other hand, we liquified grape pulp in this study. In addition to seeds, pulp also contains the other components of grape herb/fruit. Although both biomass are similar, they have more or less differences chemically. So, the behavior in the liquefaction process of two kinds of biomass is different. In this case, it is expected that the properties of these biopolyols obtained from different studies will differ from each other.

3.2.1. Hydroxyl number

The physicomechanical properties of polyurethanes can be arranged by the changes in the hydroxyl number of the polyols. In the process of liquefying biomass, liquefaction solvents are essential. These solvents, which are also polyols, must not only facilitate efficient and rapid liquefaction of biomass but also have the appropriate polyol properties for the intended PU applications. In this study, while the hydroxyl number of liquefying solvent (PEG400/G weight ratio of 4/1) was 632.6 mg KOH/g, the hydroxyl number of the control experiment, which is the reaction performed at the center point (0 level in Table 1) with liquefying solvent without GP powder, was determined as 406.2 mg KOH/g. The reduction in the hydroxyl group can be related to the dehydration of water molecules [5].

Figure 4 depicts the influences of the liquefaction reaction parameters on the hydroxyl numbers of the obtained biopolyols. The reaction time and temperature were the determinant parameters for the reactions carried out at 3% wt of catalyst (SA). For instance, when the reaction temperature was raised from 150 °C to 170 °C for 40 min reactions, the hydroxyl numbers of biopolyols started to decline. However, when the time was increased from 40 min to 80 min for both 150 °C and 170 °C reactions, the increases in the hydroxyl number were detected (Figure 4a). The hydroxyl number of 469.74 mg KOH/g was the highest and it was detected as the reaction parameters were 2 wt% SA, 60 min, and 160 °C. The hydroxyl numbers decreased as the reaction time increased gradually (20, 60, and 100 min) at the parameters of 4 wt% SA and 160 °C. Furthermore, when the reaction temperatures were increased for 60 min reactions, significant decreases in the hydroxyl numbers were detected (Figure 4b) As the catalyst loading was increased to 5 wt%, the opposite tendency in hydroxyl values to those of 3 wt% was observed.

When the reaction time was increased from 40 min to 80 min for both 150 °C and 170 °C reactions, the decreases in the hydroxyl number were determined (Figure 4c). It can be concluded from the results that all the reaction parameters have distinct influences on the hydroxyl numbers of biopolyols. The average hydroxyl number of biopolyols obtained from the validation parameters (4.25 wt% SA, 50 min, and 165 °C) was detected as 470.5 mg KOH/g. As a result, considering their hydroxyl number values, all biopolyols obtained in this study are suitable candidate raw materials to produce RPUFs used in sectors such as sandwich panel production, the refrigeration industry, furniture, automotive, etc. [20, 21].

Figure 4

3.2.2. Acid number

One of the other significant parameters affecting the polymerization reaction kinetics is the acid number of polyols. The nature of biopolyols synthesized via ACSL is acidic because the acidic catalyst is used in the method. Before fabricating RPUF, the acidity of biopolyol must be decreased using basic solutions of NaOH and Na_2CO_3 to obtain RPUFs with fine cellular structure [22, 23]. Therefore, it is desired that the acid number of biopolyol is less than 5 mg KOH/g during producing RPUF [20].

Figure 5 displays the influences of the liquefaction reaction parameters on the acid numbers of the obtained biopolyols. In this study, the acid number was found to be 32.11 mg KOH/g for the control experiment. As displayed in Figure 5a, when the reaction temperature was raised from 150 °C to 170 °C for 40 min and 3 wt% SA reactions, the acid numbers of biopolyols decreased. However, in the same temperature conditions for

80 min and 3 wt% SA reactions, the acid numbers of biopolyols increased. The acid number of biopolyol reached the lowest value (4.85 mg KOH/g) at the parameters of 2 wt% SA, 60 minutes, and 160 °C (Figure 5c). The acid numbers decreased as the reaction time increased gradually (20, 60, and 100 min) at the parameters of 4 wt% SA and 160 °C. The acid number of 31.75 mg KOH/g was the highest and it was detected as the reaction parameters were 6 wt% SA, 60 min, and 160 °C (Figure 5c). As expected, the catalyst loading was the most effective parameter for the acid numbers of biopolyols. The average acid number of the biopolyols produced from the validation experiments was determined as 23.85 mg KOH/g. These results were close to previously reported values for the acid numbers of biopolyols. [18, 21, 24]

Figure 5

3.2.3. Viscosity

When the suitability of polyols is evaluated for the use of polyurethane foam production, viscosity is one of the other important parameters coming into prominence. Polyols with high viscosity obstruct mixing with components of RPUFs, and accordingly negatively affect the polymerization reaction.

Figure 6 indicates the influences of liquefaction reaction parameters on the viscosity values of biopolyols. The viscosity was found to be 317.5 cP for the control experiment. As illustrated in Figure 6a, when the reaction temperature was raised from 150 °C to 170 °C for 40 min and 3 wt% SA reactions, the viscosity values of biopolyols increased, whereas, in the same temperature conditions for 80 min and 3 wt% SA reactions, the viscosity values of biopolyols declined. The viscosity value caused a reduction for the

parameters of 2 wt% SA, 160 °C, and 60 min reaction. (Figure 6a). The viscosity values of the biopolyols were raised from 1445 cP to 1685 cP as the reaction time was raised from 20 min to 100 min at the parameters of 4 wt% SA and 160 °C. The viscosity values of the biopolyols raised from 1358 cP to 1703 cP as the reaction temperature was raised from 140 °C to 180 °C for the 60 min reactions (Figure 6b). When the reaction temperature was increased from 150 °C to 170 °C in the presence of 5 wt% SA, a slight increase was detected for the reaction time of 40 min, while a significant increase was observed for the reaction time of 80 min. Furthermore, the increase in the reaction time from 40 min to 80 min also increased the viscosity values under the same reaction parameters (Figure 6c). The average viscosity value of the biopolyol produced from the validation experiments was determined as 1785 cP. In conclusion, while evaluating in terms of the viscosity values, all the obtained biopolyols can be used for the polyurethane foam industry.

Figure 6

3.3. FTIR and GPC analysis

FT-IR spectra of GP, GP residue, and biopolyol synthesized in the validation experiment are presented in Figure 7. Several similar peaks are seen in the spectra of GP and GP residue because of the functional groups in the lignocellulosic structure. However, significant reductions in peak intensities for the GP residue were observed. It can be concluded that the macromolecules of GP were broken down by ACSL and then liquefied [7]. The strong peak at 3406 cm^{-1} was associated with the hydroxyl (-OH) stretching vibrations. The increase in vibration peak intensity also indicated the presence of a large

number of hydroxyl groups. The lignocellulosic content of GP was probably be the source of hydroxyl groups [25]. The peak at 2855 cm^{-1} of biopolyol for the C-H stretching of CH_3, CH_2, and CH groups shifted and increased, indicating that the relevant bonds stretching between the wavelengths of 3050 cm^{-1} and 2850 cm^{-1} in GP were rearranged by liquefaction [12]. The peaks at 1725 cm^{-1}, 1650 cm^{-1}, and 1470 cm^{-1} for biopolyol were attributed to the C=O stretching (the presence of liquefied structures of ester and acetyl groups in hemicellulose), aromatic C=C stretching, and aromatic C-H in-plane bending vibrations. Although their intensity varies, these absorption bands were observed at approximately the same wavelengths for GP and GP residue. Additionally, the peak intensity at 1160 cm^{-1} for biopolyol increased, indicating the formation/increase of the number of ether bonds during the liquefaction reaction [20]. The sharp peak at 1091 cm^{-1} for biopolyol was also associated with the -C-O-C- stretching vibrations. ~~The urethane linkage can be easily formed by the reaction of isocyanates with these hydroxyl groups in the biopolyol.~~

Figure 7

The GPC chromatogram of the biopolyol is shown in Figure 8. The data of GPC analysis indicated that the liquefaction mixture comprised of two major fractions with different molecular weights. The ratio of the peak areas to the total area was used to determine the percentage share of each of the individual peaks. Regarding these results, it was seen that the average molecular weight of synthesized polyol was 586 g mol^{-1}. A molecular weight value of 5180 g mol^{-1} has been reported by Shao et al. for liquefied grape seed using similar experimental conditions (solvent mixture: PEG400 and glycerol with the ratio at

4:1; catalyst: sulfuric acid ranging from 1% to 6%; liquid–solid ratios ranging from 2 to 5; reaction temperature: 100–200 °C; reaction time, 40–320 min) [12]. Comparing these results, the biopolyol obtained in this study suggests shorter carbon chains within the liquefied grape seed structure.

Figure 8

3.4. Physicomechanical and morphological properties of foams

The properties of RPUFs are mainly influenced by their cellular morphology, type of polyols and isocyanates, the amount and type of additives, the amount and type of blowing agent, and so on [26-29]. Some important properties of RPUFs were presented in Table 6.

Figure 9 shows the SEM images of RPUF and bio-based RPUF. It is seen that the cell types of the foams were polyhedron form and there is no cell destruction with the introduction of biopolyol. Also, the average cell size of the bio-based RPUF was close to that of standard RPUF. While the average cell size of the standard RPUF was 280±75 μm, and the cell size of the bio-based RPUF was 295±95 μm.

Figure 9

The insulation performance of foams is mainly determined by the values of thermal conductivity. The thermal conductivity value of RPUF was 28.4 mW/m·K, whereas the thermal conductivity value of bio-based RPUF increased to 31.3 mW/m·K when the biopolyol was replaced with a petroleum-based polyol in half amount. The decrease in

the closed-cell content probably caused to the increase in the thermal conductivity value of the bio-based RPUF. While the closed-cell content of bio-based RPUF was 71.1%, the same value for the reference RPUF was 88.8%. Nevertheless, the thermal conductivity value of bio-based RPUF is higher than that of commercial polyurethane foam (20-24 mW/m·K); however, the thermal conductivity value found in this study is much lower than polystyrene foam, polyvinyl chloride foam, and polypropylene foam [30]. In conclusion, the produced bio-based RPUF is suitable for the use of thermal insulation material.

The compressive strength value depends mostly on the apparent density of RPUFs. The higher the density, the higher the compressive strength value [31]. While the compressive strength value of RPUF was 210.8 kPa, the value for the bio-based RPUF decreased to 105.3 kPa. The reason for this reduction in the compressive strength value can be attributed to the decreasing density of bio-based RPUF. The presence of biopolyol is expected to negatively affect the compressive strength of polyurethane foam and this is commonly found in the literature [11, 32-34]. When taking all the results into account, it can be concluded that the bio-based RPUF has great potential as sustainable insulation material.

Table 6

4. Conclusion

The liquefaction of GP via the ACSL method was carried out in the presence of an acidic catalyst (SA) using PEG400/G as liquefying solvent. CCD of RSM was used as a design of experiment technique for the optimization of the liquefaction reaction parameters. The

obtained model depicted that the liquefaction reaction parameters have significant effects on the LY. Based on variance analysis (ANOVA), the catalyst loading was the most significant parameter on the LY. The accuracy and reliability of the model were demonstrated with a high regression coefficient (R^2) of 0.9859. In addition, the reliability was confirmed by the validation experiments and the absolute error was obtained as 1.48%. The biopolyol obtained from the validation experiments exhibited proper physicochemical properties to be used in the RPUF industry and had a 470.5 mg KOH/g of hydroxyl number, 2.31 mg KOH/g of acid number, and 1785 cP of viscosity at 25 °C. Using this biopolyol, a bio-based RPUF was synthesized by replacing petroleum-based polyol in half amount and its physicomechanical properties were determined. The values of thermal conductivity, closed-cell content, apparent density, and compressive strength were 31.3 mW/m·K, 71.1%, 33.4 kg/m^3, and 105.3 kPa, respectively. As a result, ACSL can be preferred for the valorization of industrial residue GP based on the biorefinery concepts, and the obtained biopolyol can be used in the formulation of polyurethanes.

Acknowledgment

This study was funded by TUBITAK 2209-A Research Project Support Programme for Undergraduate Students and Eskisehir Technical University Scientific Research Projects (Project number: 22LÖP152).

References

1. Basu P. Biomass Gasification, Pyrolysis and Torrefaction: Practical Design and Theory. Cambridge, MA, USA: Academic Press, 2018.
2. Wang Q, Tuohedi N. Polyurethane foams and bio-polyols from liquefied cotton stalk agricultural waste. Sustainability 2020; 12 (10): 4214. https://doi.org/10.3390/su12104214

3. Tran MH, Lee E. Development and optimization of solvothermal liquefaction of marine macroalgae Saccharina japonica biomass for biopolyol and biopolyurethane production. Journal of Industrial and Engineering Chemistry 2020; 81:167-177. https://doi.org/10.1016/j.jiec.2019.09.005
4. Soares B, Gama N, Freire CS, Barros-Timmons A, Brandão I et al. Spent coffee grounds as a renewable source for ecopolyols production. Journal of Chemical Technology & Biotechnology 2015; 90 (8): 1480-1488. https://doi.org/10.1002/jctb.4457
5. Soares B, Gama N, Freire C, Barros-Timmons A, Brandão I et all. Ecopolyol production from industrial cork powder via acid liquefaction using polyhydric alcohols. ACS Sustainable Chemistry & Engineering 2014; 2 (4): 846-854. https://doi.org/10.1021/sc400488c
6. Patel CM, Barot AA, Sinha VK. Utilization of some lignocellulosic agricultural residues in polyhydric alcohol liquefaction. International Journal of Chemical Sciences and Technology 2016; 1 (2): 7-13.
7. Fidan MS, Ertaş M. Optimization of liquefaction parameters of cotton burrs (Gossypium hirsutum L.) for polyurethane-type isolation foams. Kastamonu University Journal of Forestry Faculty 2020; 20 (1): 15-24. https://doi.org/10.17475/kastorman.705805
8. Serrano L, Rincón E, García A, Rodríguez J, Briones R. Bio-degradable polyurethane foams produced by liquefied polyol from wheat straw biomass. Polymers 2020; 12 (11): 2646. https://doi.org/10.3390/polym12112646
9. Zhang Q, Chen W, Qu G, Lin X, Han D et al. Liquefaction of peanut shells with cation exchange resin and sulfuric acid as dual catalyst for the subsequent synthesis of rigid polyurethane foam. Polymers 2019; 11 (6): 993. https://doi.org/10.3390/polym11060993
10 İnternet: https://arastirma.tarimorman.gov.tr/tepge/Menu/27/Tarim-Urunleri-Piyasalari
11. Gu S, Yan T, Zuo Z et al. (2022) Polyurethane foam from grape-seed-based polyol. Green Materials 10(4): 176–183
12 Qiang Shao, Hong-Qiang Li, Chong-Pin Huang, Jian Xu Biopolyol preparation from liquefaction of grape seeds, J. APPL. POLYM. SCI. 2016, DOI: 10.1002/APP.43835
13. Erdem M, Ortaç K, Erdem B, Türk H. Effect of reactive organobentonite additives to the some performance properties of rigid polyurethane foam. Gazi Üniversitesi Mühendislik Mimarlık Fakültesi Dergisi 2017; 32 (4): 1209-1220. https://doi.org/10.17341/gazimmfd.369543 (in Turkish with an abstract in English)
14. D'Souza J, Camargo R, Yan N. Biomass liquefaction and alkoxylation: A review of structural characterization methods for bio-based polyols. Polymer Reviews 2017; 57 (4): 668-694. https://doi.org/10.1080/15583724.2017.1283328
15. He Z, Wang B, Zhang B, Feng H, Kandasamy S, et al. Synergistic effect of hydrothermal Co-liquefaction of Spirulina platensis and Lignin: Optimization of operating parameters by response surface methodology. Energy 2020; 201: 117550. https://doi.org/10.1016/j.energy.2020.117550
16. Sidik DAB, Ngadi N, Amin NAS. Optimization of lignin production from empty fruit bunch via liquefaction with ionic liquid. Bioresource Technology 2013; 135: 690-696. https://doi.org/10.1016/j.biortech.2012.09.041

17. Ye L, Zhang J, Zhao J, Tu S. Liquefaction of bamboo shoot shell for the production of polyols. Bioresource Technology 2014; 153: 147-153. https://doi.org/10.1016/j.biortech.2013.11.070
18. Hu S, Wan C, Li Y. Production and characterization of biopolyols and polyurethane foams from crude glycerol based liquefaction of soybean straw. Bioresource Technology 2012; 103 (1): 227-233. https://doi.org/10.1016/j.biortech.2011.09.125
19. Lee Y, Lee EY. Thermochemical conversion of red pine wood, Pinus densiflora to biopolyol using biobutanediol-mediated solvolysis for biopolyurethane preparation. Wood Science and Technology 2018; 52: 581-596. https://doi.org/10.1007/s00226-017-0969-7
20. Erdem M, Akdogan E, Bekki A. Optimization and characterization studies on ecopolyol production from solvothermal acid-catalyzed liquefaction of sugar beet pulp using response surface methodology. Biomass Conversion and Biorefinery 2021; 1-16. https://doi.org/10.1007/s13399-021-01579-7
21. Hu S, Luo X, Li Y: Polyols and polyurethanes from the liquefaction of lignocellulosic biomass. ChemSusChem 2014, 7(1):66-72.
22. Amran UA, Zakaria S, Chia CH, Roslan R, Jaafar SNS et al. Polyols and rigid polyurethane foams derived from liquefied lignocellulosic and cellulosic biomass. Cellulose 2019; 26: 3231-3246. https://doi.org/10.1007/s10570-019-02271-w
23. Kosmela P, Gosz K, Kazimierski P, Hejna A, Haponiuk JT et al. Chemical structures, rheological and physical properties of biopolyols prepared via solvothermal liquefaction of Enteromorpha and Zostera marina biomass. Cellulose 2019; 26: 5893-5912. https://doi.org/10.1007/s10570-019-02540-8
24. Luo X, Hu S, Zhang X, Li Y. Thermochemical conversion of crude glycerol to biopolyols for the production of polyurethane foams. Bioresource Technology 2013; 139: 323-329. https://doi.org/10.1016/j.biortech.2013.04.011
25. Huang X-Y, Li F, Xie J-L, Cornelis F, Hse C-Y et al. Microwave-assisted liquefaction of rape straw for the production of bio-oils. BioResources 2017; 12 (1): 1968-1981. https://doi.org/10.15376/biores.12.1.1968-1981
26. Brondi C, Maio ED, Bertucelli L, Parenti V, Mosciatti T. The effect of organofluorine additives on the morphology, thermal conductivity and mechanical properties of rigid polyurethane and polyisocyanurate foams. Journal of Cellular Plastics 2022; 58 (1): 121-137. https://doi.org/10.1177/0021955X20987152
27. Soykan U, Kaya S. Role of hemp fiber addition on thermal stability, heat insulation, air permeability and cellular structural features of rigid polyurethane foam. Cellular Polymers 2023; 42 (2): 88-104. https://doi.org/10.1177/02624893231152383
28. Akdogan E, Erdem M. Improvement in physico-mechanical and structural properties of rigid polyurethane foam composites by the addition of sugar beet pulp as a reactive filler. Journal of Polymer Research 2021; 28 (3): 80. https://doi.org/10.1007/s10965-021-02445-w
29. Danowska M, Piszczyk Ł, Strankowski M, Gazda M, Haponiuk JT. Rigid polyurethane foams modified with selected layered silicate nanofillers. Journal of Applied Polymer Science 2013; 130 (4): 2272-2281. https://doi.org/10.1002/app.39432

30. Akdogan E, Erdem M. Environmentally-benign rigid polyurethane foam produced from a reactive and phosphorus-functionalized biopolyol: Assessment of physicomechanical and flame-retardant properties. Reactive and Functional Polymers 2022; 177: 105320. https://doi.org/10.1016/j.reactfunctpolym.2022.105320
31. Bo G, Xu X, Tian X, Wu J, He X, et al. Synthesis and characterization of flame-retardant rigid polyurethane foams derived from gutter oil biodiesel. European Polymer Journal 2021; 147: 110329. https://doi.org/10.1016/j.eurpolymj.2021.110329
32. Akdogan E, Erdem M. A comprehensive research of low-density bio-based rigid polyurethane foams from sugar beet pulp-based biopolyol: From closed-cell towards open-cell structure, Industrial Crops & Products 2023; 200, 116809
33. Zhang J, Hori N, Takemura N. Optimization of agricultural wastes liquefaction process and preparing biobased polyurethane foams by the obtained polyols, Industrial Crops & Products 2019; 138, 111455
34. Domingos I, Ferreira J, Cruz-Lopes L, Esteves B. Polyurethane foams from liquefied orange peel wastes, Food and Bioproducts Processing 2019; 115, 223–229.

Table 1. Experimental range and the levels of independent variables

Independent variables	Symbol	Range and levels				
		-2 (α)	-1	0	1	2 (α)
Catalyst loading (wt %)	X_1	2	3	4	5	6
Reaction time (min)	X_2	20	40	60	80	100
Reaction temperature (°C)	X_3	140	150	160	170	150

Table 2. Experimental CCD matrix for the production of biopolyols along with the corresponding responses.

Order	Independent variables						Response (Experimental)	Response (Predicted)
	Real values			Coded values				
	X_1	X_2	X_3	X_1	X_2	X_3	LY (%)	LY (%)
1	3	40	150	-1	-1	-1	64.4	62.9
2*	5	40	150	1	-1	-1	73.7	-
3	3	80	150	-1	1	-1	71.3	70.9
4	5	80	150	1	1	-1	79.1	78.6
5	3	40	170	-1	-1	1	74.7	72.8
6	5	40	170	1	-1	1	85.6	86.2
7	3	80	170	-1	1	1	74.7	74.9
8	5	80	170	1	1	1	89.0	88.2
9	4	60	160	0	0	0	76.4	77.2
10	4	60	160	0	0	0	77.0	77.2
11	2	60	160	-2	0	0	59.4	60.6
12	6	60	160	2	0	0	81.9	81.7
13	4	20	160	0	-2	0	70.8	72.1
14	4	100	160	0	2	0	81.5	82.2
15	4	60	140	0	0	-2	66.5	67.4
16	4	60	180	0	0	2	86.2	86.9

17	4	60	160	0	0	0	78.5	77.2

*This experiment was considered an outlier to obtain a more robust model.

Table 3. Formulation of biopolyol-based RPUF

Components	Amounts (g)	
	RPUF	bio-based RPUF
Petroleum-based polyol	60	30
Biopolyol	-	30
pMDI	93.70	93.70
Water	1.8	1.8
Amine catalyst	0.42	0.42
Tin catalyst	0.12	0.12
Surfactant	1.2	1.2

Table 4. ANOVA of quadratic model for liquefaction yield

Source	Model					Remarks
	DF	Adj SS	Adj MS	F-test	p-test	
Model	6	985.676	164.276	104.55	0.000	Significant
X_1	3	395.697	305.525	194.44	0.000	Significant
X_2	1	89.126	89.126	251.83	0.000	Significant
X_3	1	336.166	336.166	56.72	0.000	Significant
X_1^2	1	56.721	56.721	213.94	0.000	Significant
X_2^2	1	1.197	1.197	0.83	0.398	
X_3^2	1	0.793	0.793	0.55	0.487	
X_1X_2	1	4.130	4.130	2.86	0.142	
X_1X_3	1	12.512	12.512	7.96	0.020	Significant
X_2X_3	1	14.148	14.128	8.99	0.015	Significant
Error	9	14.142	1.571			
Lack of fit	7	11.920	1.703	1.53	0.450	Not significant
Pure error	2	2.222	1.111			
Total	15	999.817				
				R^2=0.9859, Adjusted R^2=0.9764 Predicted R^2=0.9426		

Table 5. Validation of the model

Exp.	X_1 (%)	X_2 (min.)	X_3 (°C)	Liquefaction yield (%)	Error (%)
Predicted	4.25	50	165	80.1	1.48
Experimental				81.3±1.5	

Table 6. Some important properties of RPUF and bio-based RPUF

Sample	Thermal conductivity (mW/m·K)	Closed cell content (%)	Compressive strength (kPa)	Density (kg/m^3)
Bio-based RFUF	31.3±0.22	71.1±3.1	105.3±7.8	31.2±2.9
RPUF	28.4±0.32	88.8±2.2	210.8±11.2	39.0±1.3

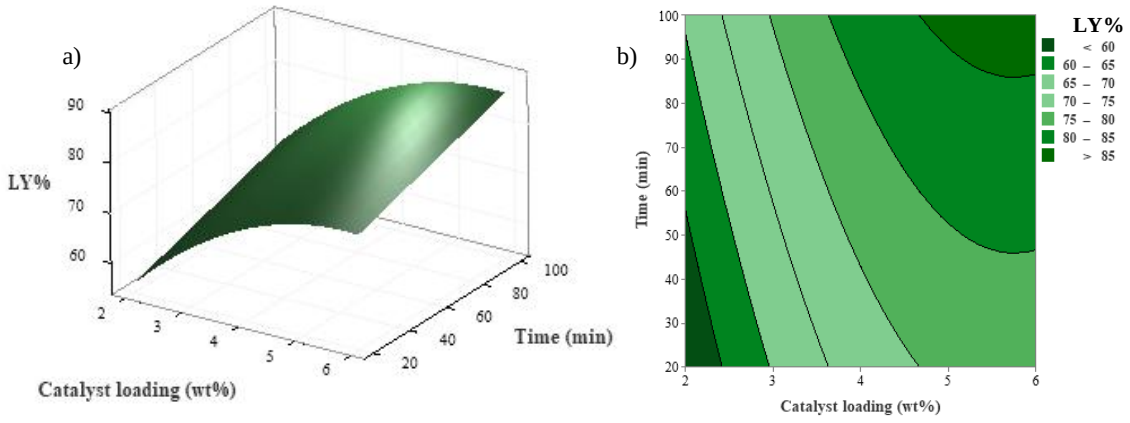

Figure 1. Combined effect of catalyst loading and reaction time on LY at constant temperature (T=160°C), a) 3D surface b) contour plots

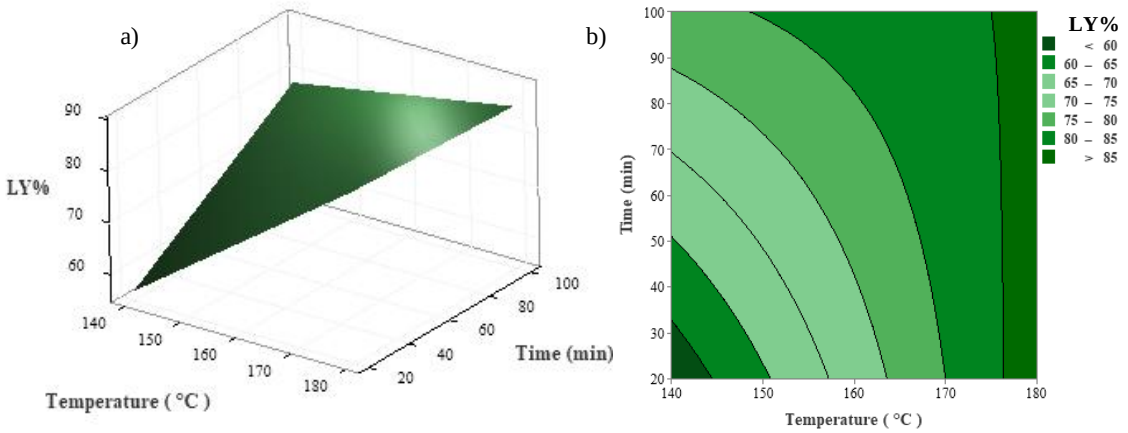

Figure 2. Combined effect of reaction temperature and reaction time on LY at a constant amount of catalyst (4%), a) 3D surface b) contour plots

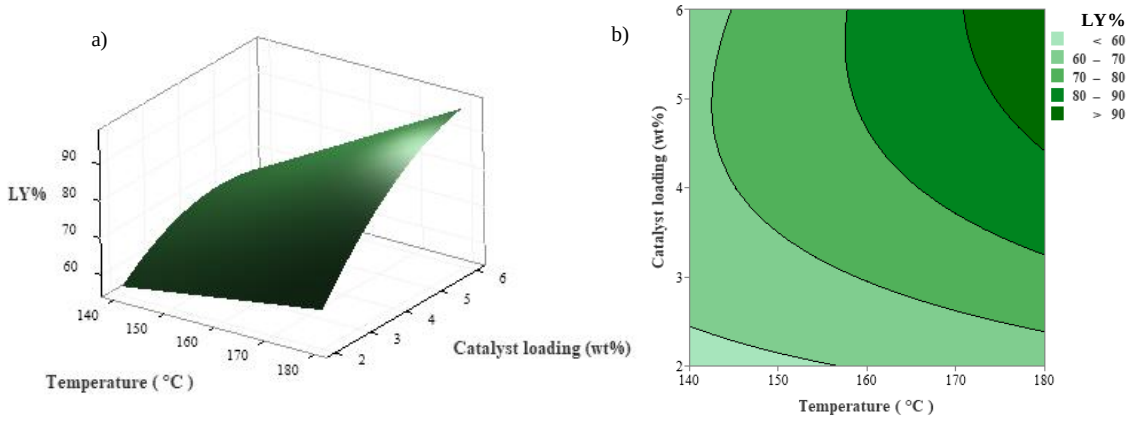

Figure 3. Combined effect of reaction temperature and catalyst loading on LY at a constant reaction time (60 min), a) 3D surface b) contour plots

1

2

3

4

5

6

7

8

9

10

11

12

13

14

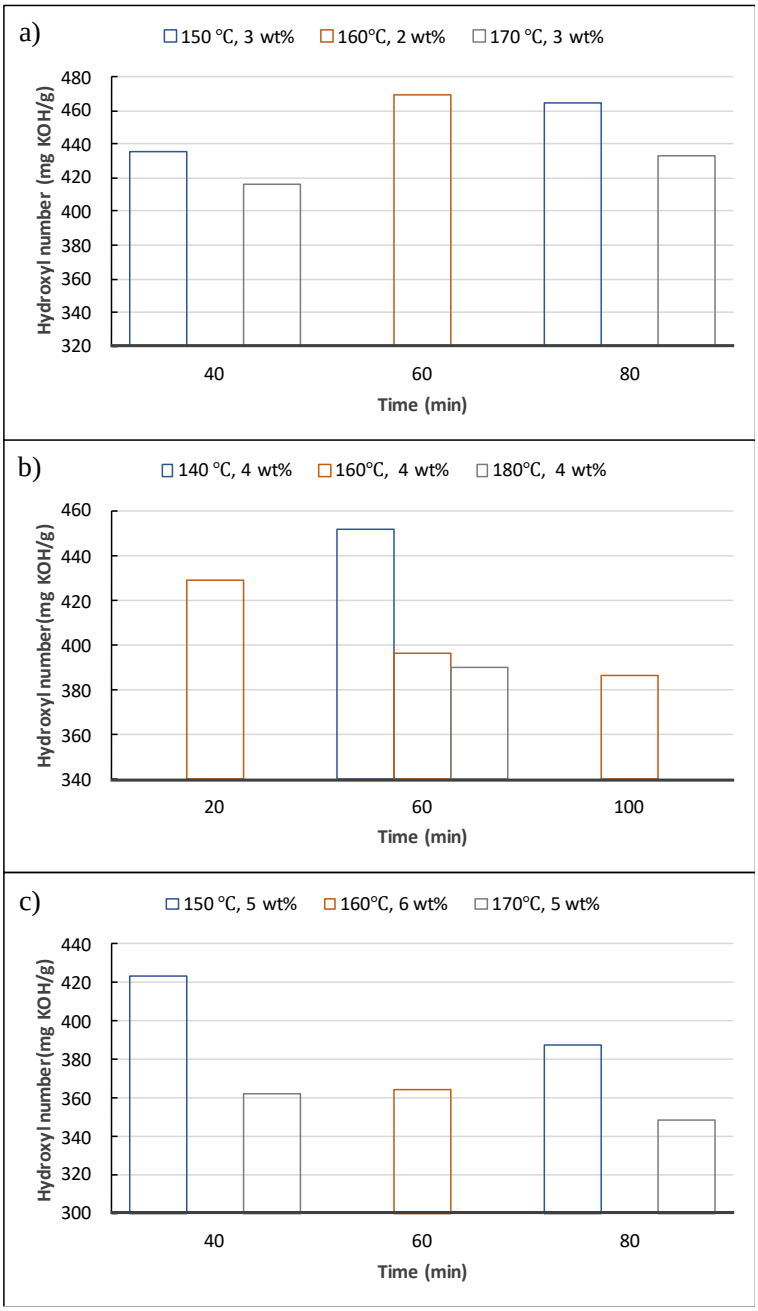

Figure 4. Effects of liquefaction reaction parameters on the hydroxyl numbers

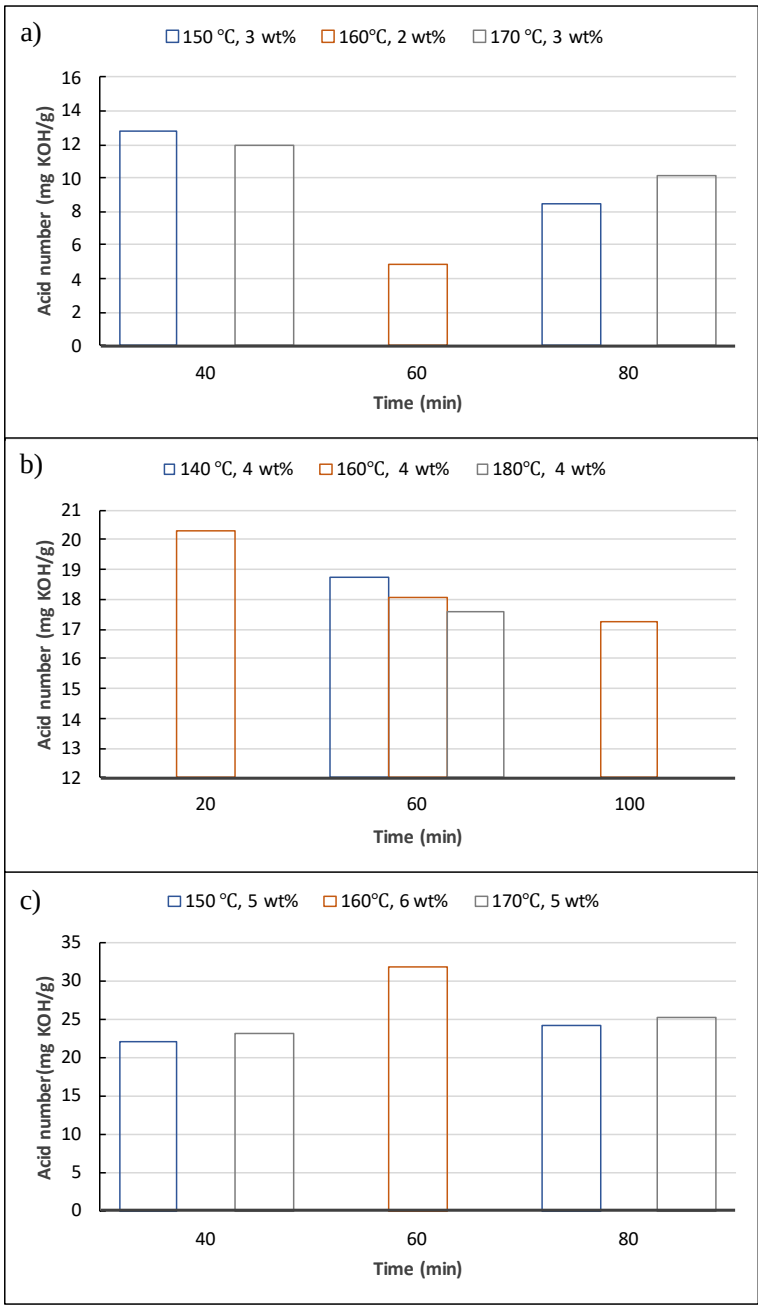

Figure 5. Effects of liquefaction reaction parameters on the acid numbers

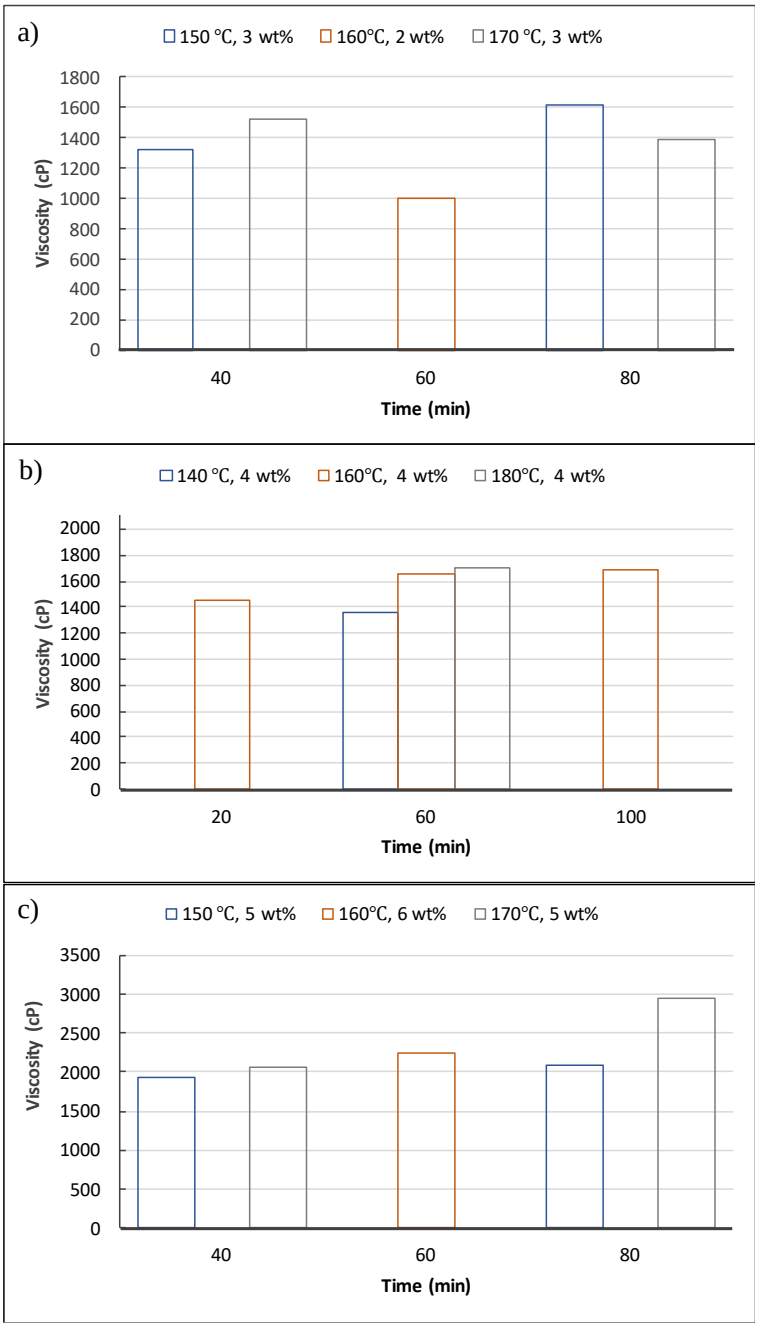

Figure 6. Effect of liquefaction reaction parameters on the viscosity values

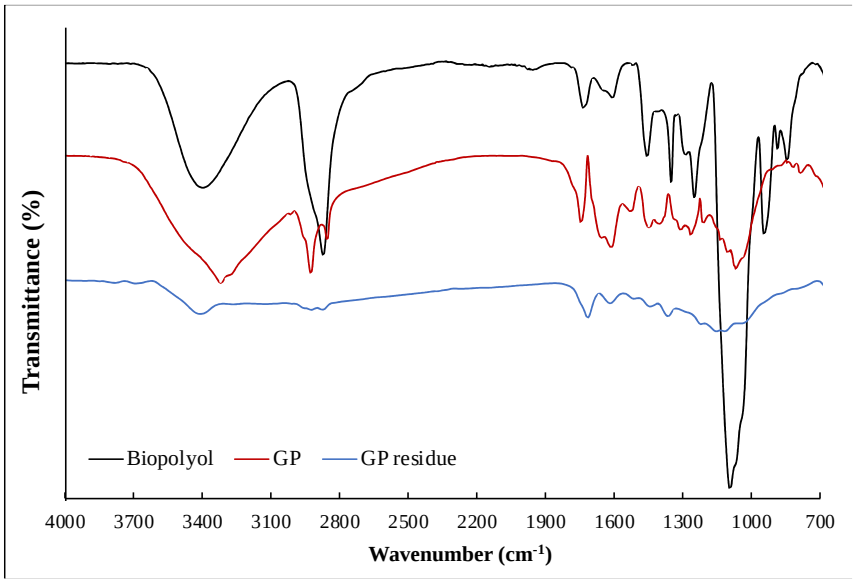

Figure 7. FT-IR spectra of GP, GP residues and biopolyol

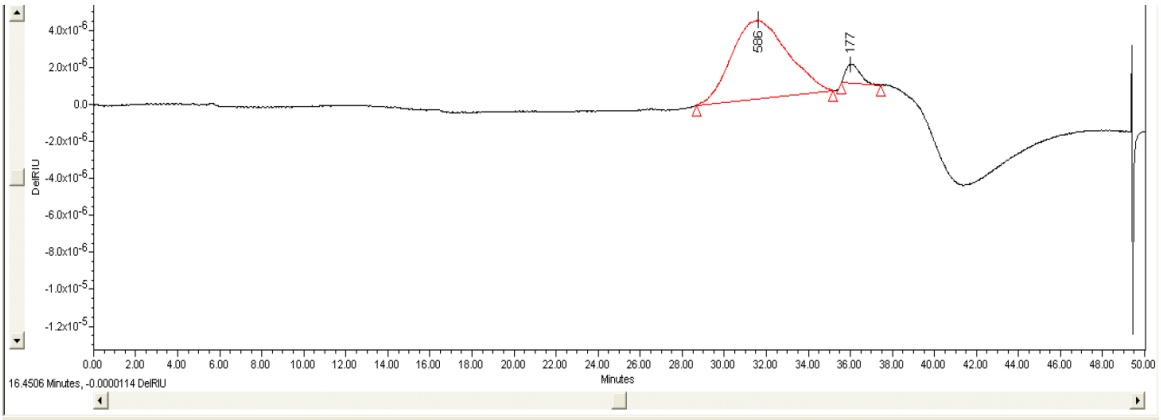

	Name	Retention Time (min)	Peak Codes	Dist Name	Mn (Daltons)	Mw (Daltons)	MP (Daltons)	Mv (Daltons)	Mz (Daltons)	Mz+1 (Daltons)	Polydispersity	[η]P (dl/g)	K (dl/g)	alpha	Mz/Mw	Mz+1/Mw	Id	Peak Sigma (mL)	System Sigma (mL)	Area (µV*sec)	% Area	Height (µV)	Int Type	MW_at_10
1		31.623					586										0			4980004	94.01	27124	bb	
2		36.007					177										0			317174	5.99	6669	bb	

Figure 8. GPC chromatogram of biopolyol

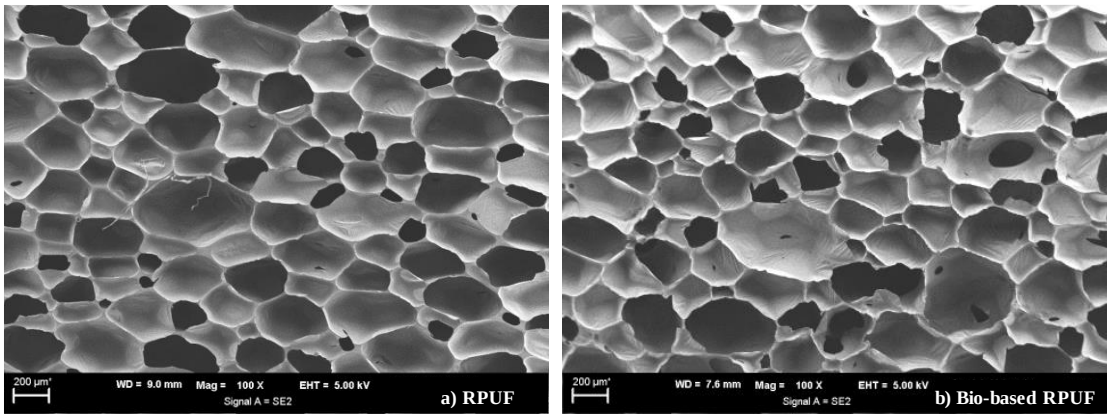

Figure 9. SEM images of foams a) RPUF and b) bio-based RPUF